

New Study of the Isotensor $\pi\pi$ Interaction

F.Q. Wu^b, B.S.Zou^{a,b,c}, L.Li^{b,d}, D.V.Bugg^e

- a) CCAST (World Laboratory), P.O. Box 8730, Beijing 100080
- b) Institute of High Energy Physics, CAS, Beijing 100039, China *
- c) Institute of Theoretical Physics, CAS, Beijing 100080, China
- d) Peking University, Beijing 100087, China
- e) Queen Mary College, London, UK

September 7, 2018

Abstract

With t-channel ρ , $f_2(1270)$ exchange and the $\pi\pi \rightarrow \rho\rho \rightarrow \pi\pi$ box diagram contribution, we reproduce the $\pi\pi$ isotensor S-wave and D-wave scattering phase shifts and inelasticities up to 2.2 GeV quite well in a K-matrix formalism. The t-channel ρ exchange provides repulsive negative phase shifts while the t-channel $f_2(1270)$ gives an attractive force to increase the phase shifts for $\pi\pi$ scattering above 1 GeV, and the coupled-channel box diagram causes the inelasticities. The implication to the isoscalar $\pi\pi$ S-wave interaction is discussed.

*mailing address, E-mail: zoubs@mail.ihep.ac.cn

1 Introduction

Much attention has been paid to the isospin $I=0$ $\pi\pi$ S-wave interaction due to its direct relation to the σ particle and the scalar glueball candidates [1, 2, 3, 4, 5, 6, 7]. However, to really understand the isoscalar $\pi\pi$ S-wave interaction, one must first understand the isospin $I=2$ $\pi\pi$ S-wave interaction due to the following two reasons: (1) There are no known s-channel resonances and less coupled channels in $I=2$ $\pi\pi$ system, so it is much simpler than the $I=0$ $\pi\pi$ S-wave interaction; (2) To extract $I=0$ $\pi\pi$ S-wave phase shifts from experimental data on $\pi^+\pi^- \rightarrow \pi^+\pi^-$ and $\pi^+\pi^- \rightarrow \pi^0\pi^0$ obtained by $\pi N \rightarrow \pi\pi N$ reactions, one needs an input of the $I=2$ $\pi\pi$ S-wave interaction.

Experimental information on the $I=2$ $\pi\pi$ scattering mainly came from $\pi^+p \rightarrow \pi^+\pi^+n$ [8] and $\pi^-d \rightarrow \pi^-\pi^-pp$ [9, 10] reactions. As shown in Fig.3, the main features for the $I=2$ $\pi\pi$ S-wave phase shifts δ_0^2 and inelasticities η_0^2 are: (1) the δ_0^2 goes down more and more negative as the $\pi\pi$ invariant mass increases from $\pi\pi$ threshold up to 1.1 GeV; (2) the δ_0^2 starts to increase for energies above about 1.1 GeV; (3) the η_0^2 starts to deviate from 1 for energies above 1.1 GeV. The first feature can be well explained by the t-channel ρ exchange force [11, 12, 13, 14, 15, 16] although it can also be reproduced by other approaches [17]. Due to the relative poor quality of the $I=2$ $\pi\pi$ scattering data above 1.1 GeV, the other two features are usually overlooked. In this paper, we show in a K-matrix formalism [12, 18] that these two features can be well reproduced by the t-channel $f_2(1270)$ exchange and the $\pi\pi$ - $\rho\rho$ coupled-channel effect, respectively.

A correct description of the $I = 2$ $\pi\pi$ S-wave interaction is important for the extraction of the $I = 0$ $\pi\pi$ S-wave interaction from experimental data. While the $I = 2$ $\pi\pi$ S-wave interaction can be extracted from the pure $I = 2$ $\pi^\pm\pi^\pm \rightarrow \pi^\pm\pi^\pm$ reactions, the $I = 0$ $\pi\pi$ S-wave interaction can only be extracted from $\pi^+\pi^- \rightarrow \pi^+\pi^-$ and $\pi^+\pi^- \rightarrow \pi^0\pi^0$ reactions which are mixture of $I = 0$ and $I = 2$ contributions. Recently, the $\pi^+\pi^- \rightarrow \pi^+\pi^-$ scattering from the old πN scattering experiments with both unpolarized[19] and polarized targets[20] has been re-analyzed[3, 21] in combination with new information from $p\bar{p}$ and other experiments. The $\pi^+\pi^- \rightarrow \pi^0\pi^0$ scattering has also been studied by E852[22] and GAMS[23] Collaborations. The relation between the $\pi^+\pi^- \rightarrow \pi^+\pi^-$, $\pi^0\pi^0$ S-wave amplitudes and the isospin decoupled amplitudes is as the following:

$$T_s(+-,+-) = T_s^{I=0}/3 + T_s^{I=2}/6, \quad (1)$$

$$T_s(+-,00) = T_s^{I=0}/3 - T_s^{I=2}/3. \quad (2)$$

Experimental information on $T_s^{I=0}$ was extracted from $T_s(+-,+-)$ and $T_s(+-,00)$ information by assuming some kind of $T_s^{I=2}$ amplitude. For example, in Refs.[3, 12, 19], a scattering length formula for $I=2$ $\pi\pi$ S-wave was used; in Ref.[6] another empirical parametrization was used. These parametrizations give similar phase shifts up to 1.1 GeV, but differ at higher energies. All these previous analyses have ignored the inelastic effects in the $I = 2$ channel. We will demonstrate that the correct description of the $I = 2$ S-wave interaction has significant impact on the extraction of the $I = 0$ $\pi\pi$ S-wave amplitude for energies above 1.1 GeV.

2 Formalism

In our normalization the S-matrix of two-body scattering takes the form

$$\langle p'_1 p'_2 | S | p_1 p_2 \rangle = I - (2\pi)^4 \delta^4(p_1 + p_2 - p'_1 - p'_2) \frac{T(p_1, p_2, p'_1, p'_2)}{(2E_1)^{\frac{1}{2}} (2E_2)^{\frac{1}{2}} (2E'_1)^{\frac{1}{2}} (2E'_2)^{\frac{1}{2}}}, \quad (3)$$

the states are normalized as

$$\langle p' | p \rangle = (2\pi)^3 \delta^3(p - p'). \quad (4)$$

Our normalization is such that the unitarity relation for partial-wave amplitudes reads:

$$\text{Im}T_1(s) = T_1^\dagger(s)\rho(s)T_1(s), \quad (5)$$

with $\rho(s)$ the diagonal matrix of phase space. Taking the $\pi\pi$ channel as channel 1, then $\rho_1(s) = (1 - 4m_\pi^2/s)^{1/2}$. The partial-wave amplitudes are obtained from the full amplitude by the standard projection formula[24, 12]

$$T_l(s) = \frac{1}{s - 4m_\pi^2} \int_{4m_\pi^2-s}^0 dt P_l(x) \left[1 + \frac{2t}{s - 4m_\pi^2} \right] T(s, t, u), \quad (6)$$

where $P_l(x)$ is Legendre function, and s, t, u are the usual Mandelstam variables. The relation between the amplitude $T_l(s)$ for $\pi\pi \rightarrow \pi\pi$ scattering and

phase shift parameters δ_l and η_l is

$$T_l^I(s) = \frac{\eta_l^I(s)e^{2i\delta_l^I(s)} - 1}{2i\rho_1(s)}. \quad (7)$$

To exhibit the isospin structure, T can be written in terms of three invariant amplitudes A , B and C by

$$T(s, t, u) = A(s, t, u)\delta_{\alpha\beta}\delta_{\gamma\delta} + B(s, t, u)\delta_{\alpha\gamma}\delta_{\beta\delta} + C(s, t, u)\delta_{\alpha\delta}\delta_{\beta\gamma}, \quad (8)$$

where α, β, γ and δ are isospin indices of pions. Using isospin projection operator leads to:

$$T^{I=0}(s, t, u) = 3A(s, t, u) + B(s, t, u) + C(s, t, u) \quad (9)$$

$$T^{I=1}(s, t, u) = B(s, t, u) - C(s, t, u) \quad (10)$$

$$T^{I=2}(s, t, u) = B(s, t, u) + C(s, t, u). \quad (11)$$

Then we follow the K -matrix formalism as in Refs.[12, 18, 15]. The K -matrix unitarization is introduced by

$$T_l^I(s) = \frac{K_l^I(s)}{1 - i\rho(s)K_l^I(s)}, \quad (12)$$

in which l is the index of partial-wave and I the index of isospin.

For the two-channel case, the two-dimensional K matrix and $\rho(s)$ matrix are

$$K = \begin{pmatrix} K_{11} & K_{12} \\ K_{12} & K_{22} \end{pmatrix}, \quad \rho(s) = \begin{pmatrix} \rho_1(s) & 0 \\ 0 & \rho_2(s) \end{pmatrix}, \quad (13)$$

where $\rho_2(s)$ is the phase space factor for $\rho\rho$ channel, K_{11} is K -matrix element for the channel of $\pi\pi \rightarrow \pi\pi$, K_{22} for the channel of $\rho\rho \rightarrow \rho\rho$, and K_{12} for $\pi\pi \rightarrow \rho\rho$. Then substituting relation Eq.(13) into $T = K/(1 - i\rho K)$, one obtains

$$T_{11} = \frac{K_{11} - i\rho_2(K_{11}K_{22} - K_{12}K_{21})}{1 - i\rho_1K_{11} - i\rho_2K_{22} - \rho_1\rho_2(K_{11}K_{22} - K_{12}K_{21})}, \quad (14)$$

Ignoring the interaction between $\rho\rho$, we have $K_{22} = 0$; then

$$T_{11} = \frac{K_{11} + iK_{12}\rho_2K_{21}}{1 - i\rho_1(K_{11} + iK_{12}\rho_2K_{21})}, \quad (15)$$

where $K_{12}\rho_2K_{21}$ corresponds to the contribution of the $\pi\pi \rightarrow \rho\rho \rightarrow \pi\pi$ box diagram. After substituting T_{11} for T_l^I in Eq.(7), we may get phase shift parameters δ and η by solving Eq.(7).

In order to obtain K_{11} , we incorporate the t -channel $f_2(1270)$ contribution into the t -channel ρ exchange term by the Dalitz-Tuan method [3, 12]. Supposing two components a and b for the partial wave l are expressed individually as

$$T_l^a(s) = \frac{G_a}{C_a(s) - iG_a\rho_1(s)} \text{ and } T_l^b(s) = \frac{G_b}{C_b(s) - iG_b\rho_1(s)},$$

then the combined amplitude will be

$$\begin{aligned} \hat{T}_l^{ab}(s) &= \frac{G_a C_b(s) + G_b C_a(s)}{[C_a(s) - iG_a\rho_1(s)][C_b(s) - iG_b\rho_1(s)]} \\ &= \frac{G_{ab}}{C_{ab}(s) - iG_{ab}\rho_1(s)}, \end{aligned} \quad (16)$$

with $C_{ab}(s) = C_a(s)C_b(s) - G_a G_b \rho_1^2(s)$, and $G_{ab} = G_a C_b(s) + G_b C_a(s)$. The amplitude is explicitly unitary, and the denominator contains the same poles as in each component. Further poles are added one by one using the equations above. For example, the combination of the t -channel ρ exchange and the f_2 exchange gives

$$K_{11} = \frac{K_\rho(s) + K_{f_2}(s)}{1 - \rho_1^2(s)K_\rho(s)K_{f_2}(s)}. \quad (17)$$

2.1 t -channel ρ meson exchange amplitude

This section has been partially presented in Ref.[12]. We start with the Born term of the $\pi\pi$ scattering amplitude by ρ exchange

$$T^{Born}(I=0) = 2G_{\pi\pi\rho} \left[\left(\frac{\Lambda^2 - m_\rho^2}{\Lambda^2 - t} \right)^2 \frac{s-u}{m_\rho^2 - t} + \left(\frac{\Lambda^2 - m_\rho^2}{\Lambda^2 - u} \right)^2 \frac{s-t}{m_\rho^2 - u} \right], \quad (18)$$

$$T^{Born}(I=2) = -\frac{1}{2}T^{Born}(I=0), \quad (19)$$

where $G_{\pi\pi\rho} = g_{\pi\pi\rho}^2/32\pi=0.364$, and at each vertex we have used a form factor of conventional monopole type to take into account the off-shell behavior of

the exchanged mesons:

$$F(q^2) = \frac{\Lambda^2 - m^2}{\Lambda^2 - q^2}, \quad (20)$$

where m and q are the mass and four-vector momentum, respectively, of exchanged mesons, and Λ is the cutoff parameter to be determined by experimental data.

Their S-wave projections are

$$K_S^{I=0}(s) = 4G_{\pi\pi\rho} \left\{ \left(\frac{m_\rho^2}{\Lambda^2} - 1 \right) \frac{\Lambda^2 + 2s - 4m_\pi^2}{\Lambda^2 + s - 4m_\pi^2} + \frac{2s + m_\rho^2 - 4m_\pi^2}{s - 4m_\pi^2} \ln \frac{(s + m_\rho^2 - 4m_\pi^2)\Lambda^2}{(s + \Lambda^2 - 4m_\pi^2)m_\rho^2} \right\}, \quad (21)$$

$$K_S^{I=2}(s) = -\frac{1}{2} K_S^{I=0}(s). \quad (22)$$

Their I=2 D-wave projection is

$$\begin{aligned} K_D^{I=2}(s) = & \frac{2G_{\pi\pi\rho}(\Lambda^2 - m_\rho^2)}{\Lambda^2(s - 4m_\pi^2)^2(\Lambda^2 + s - 4m_\pi^2)} \left\{ 12\Lambda^6 - 6\Lambda^4(12m_\pi^2 + m_\rho^2 - 4s) \right. \\ & + \Lambda^2(28m_\pi^2 + 6m_\rho^2 - 13s)(4m_\pi^2 - s) - 2(2m_\pi^2 - s)(s - 4m_\pi^2)^2 \left. \right\} \\ & + \frac{G_{\pi\pi\rho}}{(4m_\pi^2 - s)^2} \left\{ 2 \left[12\Lambda^6 + 12\Lambda^2 m_\rho^2(8m_\pi^2 - 3s) - 6\Lambda^4(8m_\pi^2 + 3m_\rho^2 \right. \right. \\ & - 3s) + (4m_\pi^2 - s)[16m_\pi^4 + s(13m_\rho^2 + 2s) - 4m_\pi^2(7m_\rho^2 + 3s)] \ln(1 + \\ & \left. \left. \frac{s - 4m_\pi^2}{\Lambda^2}) - 2(4m_\pi^2 - m_\rho^2 - 2s)[16m_\pi^4 + 6m_\rho^4 + 6m_\rho^2 s + s^2 \right. \right. \\ & \left. \left. - 8m_\pi^2(3m_\rho^2 + s) \right] \ln(1 + \frac{s - 4m_\pi^2}{m_\rho^2}) \right\}. \quad (23) \end{aligned}$$

2.2 t -channel $f_2(1270)$ meson exchange amplitude

The amplitude for the t -channel $f_2(1270)$ meson exchange without considering the vertex form factor was given in Ref.[13] for studying $I = 0$ $\pi\pi$ scattering. Here we include the form factor to take into account the off-shell behavior of the exchanged f_2 meson. Then the Born amplitudes for the

t -channel f_2 exchange are

$$\begin{aligned}
T^{Born}(I=0) &= G_{\pi\pi f_2} \left[\frac{3(t-u)^2 - (4m_\pi^2 - s)^2}{m_{f_2}^2 - s} \left(\frac{\Lambda^2 + m_{f_2}^2}{\Lambda^2 + s} \right)^2 + \right. \\
&\quad \frac{(s-u)^2 - (4m_\pi^2 - t)^2/3}{m_{f_2}^2 - t} \left(\frac{\Lambda^2 - m_{f_2}^2}{\Lambda^2 - t} \right)^2 + \\
&\quad \left. \frac{(s-t)^2 - (4m_\pi^2 - u)^2/3}{m_{f_2}^2 - u} \left(\frac{\Lambda^2 - m_{f_2}^2}{\Lambda^2 - u} \right)^2 \right], \quad (24)
\end{aligned}$$

$$\begin{aligned}
T^{Born}(I=2) &= G_{\pi\pi f_2} \left[\frac{(s-u)^2 - (4m_\pi^2 - t)^2/3}{m_{f_2}^2 - t} \left(\frac{\Lambda^2 - m_{f_2}^2}{\Lambda^2 - t} \right)^2 + \right. \\
&\quad \left. \frac{(s-t)^2 - (4m_\pi^2 - u)^2/3}{m_{f_2}^2 - u} \left(\frac{\Lambda^2 - m_{f_2}^2}{\Lambda^2 - u} \right)^2 \right], \quad (25)
\end{aligned}$$

with $G_{\pi\pi f_2} \simeq 0.19 \text{ GeV}^{-2}$ determined from the width of $f_2(1270)$.

Their S-wave projections are

$$\begin{aligned}
K_{f_2}^{I=0} &= K_{f_2}^{I=2} \\
&= G_{\pi\pi f_2} \left\{ \frac{\frac{4}{3}(m_{f_2}^2 - \Lambda^2)(\Lambda^4 + 6\Lambda^2 s - 8\Lambda^2 m_\pi^2 + 6s^2 - 24sm_\pi^2 + 16m_\pi^4)}{\Lambda^2(\Lambda^2 + s - 4m_\pi^2)} \right. \\
&\quad + \frac{2[(2s + m_{f_2}^2 - 4m_\pi^2)^2 - (m_{f_2}^2 - 4m_\pi^2)^2/3]}{s - 4m_\pi^2} \ln\left[1 + \frac{s - 4m_\pi^2}{m_{f_2}^2}\right] \\
&\quad + \frac{\frac{4}{3}(\Lambda^4 - 2\Lambda^2 m_{f_2}^2 - 6s^2 + 24sm_\pi^2 - 6sm_{f_2}^2 - 16m_\pi^4 + 8m_{f_2}^2 m_\pi^2)}{s - 4m_\pi^2} \times \\
&\quad \left. \ln\left[1 + \frac{s - 4m_\pi^2}{\Lambda^2}\right] \right\}. \quad (26)
\end{aligned}$$

Their I=2 D-wave projection is

$$\begin{aligned}
K_D^{I=2}(s) &= \frac{2G_{\pi\pi f_2}}{3\Lambda^2(4m_\pi^2 - s)^3(\Lambda^2 - 4m_\pi^2 + s)} \left\{ -2(\Lambda^2 - m_{f_2}^2)(4m_\pi^2 - \right. \\
&\quad s) \left[18\Lambda^8 - 3\Lambda^6(60m_\pi^2 + 2m_{f_2}^2 - 31s) + 2(-4m_\pi^2 + s)^2(8m_\pi^4 \right. \\
&\quad \left. - 12m_\pi^2 s + 3s^2) - \Lambda^2(4m_\pi^2 - s)(128m_\pi^4 - 6m_{f_2}^4 + \right. \\
&\quad \left. 4m_\pi^2(15m_{f_2}^2 - 44s) - 39m_{f_2}^2 s + 42s^2) + \Lambda^4(544m_\pi^4 - \right.
\end{aligned}$$

$$\begin{aligned}
& 6m_{f_2}^4 + 28m_\pi^2(3m_{f_2}^2 - 20s) - 45m_{f_2}^2s + 112s^2) \Big] + 2\Lambda^2(\Lambda^2 - \\
& 4m_\pi^2 + s) \left[\left(18\Lambda^8 - 12\Lambda^6(12m_\pi^2 + 2m_{f_2}^2 - 7s) - \right. \right. \\
& 2\Lambda^2m_{f_2}^2(304m_\pi^4 - 344m_\pi^2s + 73s^2) - 2(4m_\pi^2 - s)(32m_\pi^6 - \\
& 3s^2(7m_{f_2}^2 + s) + 8m_\pi^2s(11m_{f_2}^2 + 3s) - 8m_\pi^4(8m_{f_2}^2 + 7s)) + \\
& \Lambda^4(304m_\pi^4 + 8m_\pi^2(27m_{f_2}^2 - 43s) + s(-126m_{f_2}^2 + \\
& 73s)) \Big) \log\left[\frac{\Lambda^2}{\Lambda^2 - 4m_\pi^2 - s}\right] + \left((-4m_\pi^2 + m_{f_2}^2)^2 + 6(-4m_\pi^2 + \\
& m_{f_2}^2)s + 6s^2 \right) \left(16m_\pi^4 + 6m_{f_2}^4 + 6m_{f_2}^2s + s^2 - 8m_\pi^2(3m_{f_2}^2 + \right. \\
& \left. s) \right) \log\left[\frac{m_{f_2}^2}{m_{f_2}^2 - 4m_\pi^2 + s}\right] \Big] \Big\}. \tag{27}
\end{aligned}$$

2.3 The $\pi\pi \rightarrow \rho\rho \rightarrow \pi\pi$ box diagram amplitude

For energies above the $\rho\rho$ threshold, the inelastic effect should be taken into account in the $I = 2$ $\pi\pi$ channel. Note that unlike $I = 0$ $\pi\pi$ channel, the $I = 2$ $\pi\pi$ channel does not couple to the $K\bar{K}$ channel due to isospin conservation. The $\pi\pi$ channel couples to the $\rho\rho$ channel by the t-channel π exchange as shown in Fig.1.

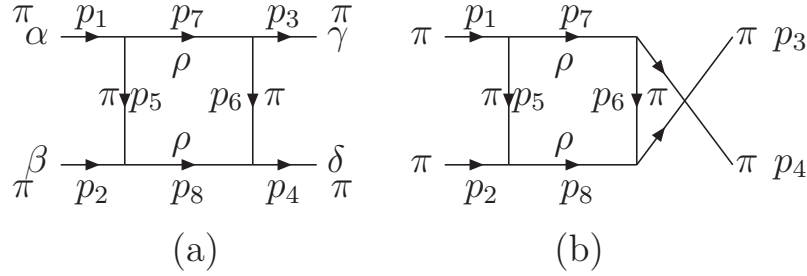


Figure 1: The $\pi\pi \rightarrow \rho\rho \rightarrow \pi\pi$ box diagrams

Assuming the on-shell approximation [25] for the $\rho\rho$ intermediate state, the Lorentz-invariant matrix element \mathcal{M} of the box diagram (Fig.1(a)) is

$$i\mathcal{M}_a = -\frac{1}{64\pi^2} \cdot \rho_2 \cdot g_{\pi\pi\rho}^4 \int d\Omega_7 \left[-(p_1 + p_5) \cdot (p_3 - p_6) + \right.$$

$$\left. \frac{(p_1 + p_5) \cdot p_7 \cdot p_7 \cdot (p_3 - p_6)}{m_\rho^2} \right]^2 \cdot \frac{1}{(p_5^2 - m_\pi^2)(p_6^2 - m_\pi^2)} \cdot (\delta_{\alpha\beta}\delta_{\gamma\delta} + \delta_{\alpha\gamma}\delta_{\beta\delta}), \quad (28)$$

where we have used the Cutkosky rule [26]. α, β, γ and δ are their isospin indices. The box diagram contribution includes Fig.1 (a) and Fig.1 (b). Fig.1 (b) gives the same amplitude as Fig.1 (a), so we have $\mathcal{M} = \mathcal{M}_a + \mathcal{M}_b = 2\mathcal{M}_a$. In our convention, $T = \mathcal{M}/(32\pi)$. After including the vertex form factors to take into account the off-shell behavior of the exchanged pions, its $I = 2$ S-wave projection is

$$\begin{aligned} T_s^{I=2} &= \frac{1}{2} \int d \cos \theta_3 T \\ &= i \cdot \frac{G_{\pi\pi\rho}^2}{2\pi} \cdot \rho_2 \cdot \int d \cos \theta_3 d \cos \theta_7 d \phi_7 \left[- (p_1 + p_5) \cdot (p_3 - p_6) + \right. \\ &\quad \left. \frac{(p_1 + p_5) \cdot p_7 \cdot p_7 \cdot (p_3 - p_6)}{m_\rho^2} \right]^2 \cdot \frac{1}{(p_5^2 - m_\pi^2)(p_6^2 - m_\pi^2)} \\ &\quad \cdot \left(\frac{\Lambda_{\pi\pi\rho}^2 - m_\pi^2}{\Lambda_{\pi\pi\rho}^2 - p_5^2} \right)^2 \cdot \left(\frac{\Lambda_{\pi\pi\rho}^2 - m_\pi^2}{\Lambda_{\pi\pi\rho}^2 - p_6^2} \right)^2 \end{aligned} \quad (29)$$

with $G_{\pi\pi\rho} = g_{\pi\pi\rho}^2/(32\pi) = 0.364$. This box diagram amplitude is related to the K-matrix element K_{12} as

$$T_s^{I=2} = iK_{12}\rho_2K_{12}. \quad (30)$$

The ρ_2 is the phase space for $\rho\rho$. If we ignore the width of the ρ meson to treat it as a stable particle, the ρ_2 in our convention can be written as

$$\begin{aligned} \rho_2^{stable}(s) &= (8\pi) \cdot (2\pi)^4 \int \delta^4(p - p_{\rho_1} - p_{\rho_2}) \frac{d^3p_{\rho_1}}{(2\pi)^3 2E_{\rho_1}} \frac{d^3p_{\rho_2}}{(2\pi)^3 2E_{\rho_2}} \\ &= \frac{2|p_\rho|}{\sqrt{s}} = \sqrt{1 - \frac{4M_\rho^2}{s}}. \end{aligned} \quad (31)$$

Taking into account the width of the ρ meson, Γ_ρ , then the phase space factor should be

$$\begin{aligned} \rho_2(s) &= \frac{1}{\pi^2} \int ds_{12} ds_{34} \frac{M_\rho \Gamma_\rho}{(M_\rho^2 - s_{12})^2 + (M_\rho \Gamma_\rho)^2} \cdot \frac{M_\rho \Gamma_\rho}{(M_\rho^2 - s_{34})^2 + (M_\rho \Gamma_\rho)^2} \\ &\quad \cdot \frac{\sqrt{[s - (\sqrt{s_{12}} + \sqrt{s_{34}})^2][s - (\sqrt{s_{12}} - \sqrt{s_{34}})^2]}}{s}. \end{aligned} \quad (32)$$

In order to get analytic formula of $\rho_2(s)$ for convenience of application, we use the following formula to fit $\rho_2(s)$ obtained numerically by Eq.(32)

$$\rho_2(s) = \frac{\sqrt{1 - \frac{1}{s}}}{1 + e^{a_1 s^3 + a_2 s^2 + a_3 s + a_4}} \quad (33)$$

where a_1, a_2, a_3 and a_4 are parameters with fitted values as $a_1 = -0.0888, a_2 = 1.3337, a_3 = -6.9465, a_4 = 11.5204$. This analytic formula for $\rho_2(s)$ is used in our final calculation. Fig.2 shows the comparison of this analytic formula (solid line) with those given by Eq.(31) (dot-dashed line) and Eq.(33) (dashed line).

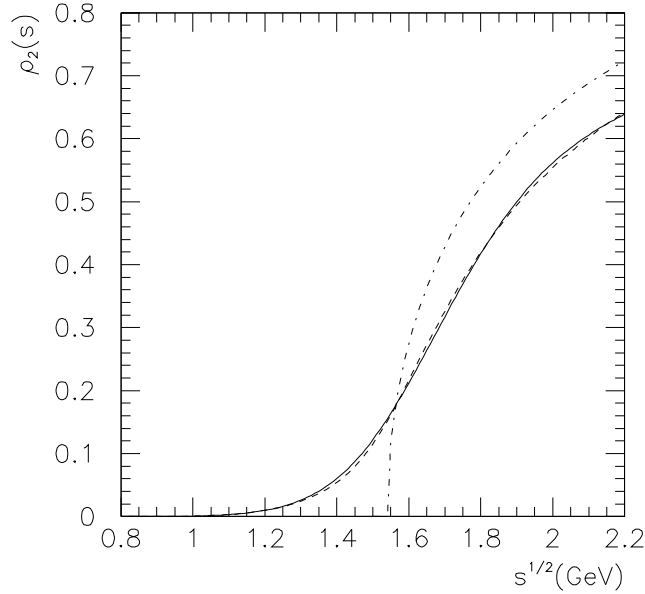


Figure 2: Comparison of $\rho\rho$ phase space $\rho_2(s)$ given by Eq.(31) (dot-dashed line), Eq.(32) (dashed line) and Eq.(33) (solid line).

3 Numerical results and discussion

From the formalism given above, we get $I=2$ $\pi\pi$ S-wave and D-wave phase shifts and inelasticities as shown in Fig.3 and Fig.4. The t-channel ρ exchange alone (dashed lines) reproduces the phase shifts for energies up to 1.1 GeV very well with the form factor parameter $\Lambda_{\rho\pi\pi} = 1.5$ GeV [12], but underestimates the phase shifts at higher energies. The inclusion of the t-channel $f_2(1270)$ exchange increases the phase shifts especially for energies above 1 GeV and can reproduce the phase shift data very well with the form factor parameter $\Lambda_{f_2\pi\pi} = 1.7$ GeV as shown by the dot-dashed lines. However the t-channel ρ and f_2 exchange only contribute to the elastic scattering and cannot produce the inelasticities for energies above 1 GeV.

The experimental information on the inelasticities is scarce for the $I = 2$ $\pi\pi$ scattering. Two data points were given by Ref.[10] for energies 1 \sim 1.5 GeV. For energies 1.5 \sim 2 GeV, Ref.[9] estimated to be 0.5 ± 0.2 for the η_0^2 in one solution and assumed $\eta_0^2 = 1.53 - 0.475m_{\pi\pi}$ (GeV/ c^2) for another solution. The two solutions gave similar results for the $I = 2$ $\pi\pi$ S-wave phase shifts. For the $I = 2$ $\pi\pi$ D-wave scattering, the inelasticity could not be measured well and was ignored, *i.e.*, assuming $\eta_2^2 = 1$ for the extraction of the δ_2^2 shown in Fig.4.

Although there are only three data points with large error bars for the inelasticity parameter η_0^2 of the $I = 2$ $\pi\pi$ S-wave scattering, it is clear that the inelastic effect may be significant around 1.6 GeV. In order to reproduce this inelasticity, it is necessary to consider the $\pi\pi \leftrightarrow \rho\rho$ coupling channel effect. We find that including contribution from the $\pi\pi \rightarrow \rho\rho \rightarrow \pi\pi$ box diagram in our K-matrix formalism, the $I = 2$ S-wave inelasticity data can be very well reproduced without introducing any more free parameter as shown in Fig.3(b). The same diagram also predicts a broad shallow dip around 1.7 GeV for the inelasticity of the $I = 2$ D-wave scattering as shown in Fig.4(b). Assuming $\eta_2^2 = 1$ for energies around 1.7 GeV may bias the δ_2^2 data around this energy. This may be the reason that the δ_2^2 data around 1.7 GeV has the largest discrepancy with our theoretical result. The box diagram has little influence to the phase shifts although it produces large inelasticity.

Inspired by the new discovery of a pentaquark state [27, 28, 29, 30], we also explored the possibility of including an $I = 2$ s-channel resonance to reproduce the $I = 2$ $\pi\pi$ S-wave scattering data instead of using the t-channel f_2 exchange and the $\pi\pi \rightarrow \rho\rho \rightarrow \pi\pi$ box diagram, but failed to reproduce the

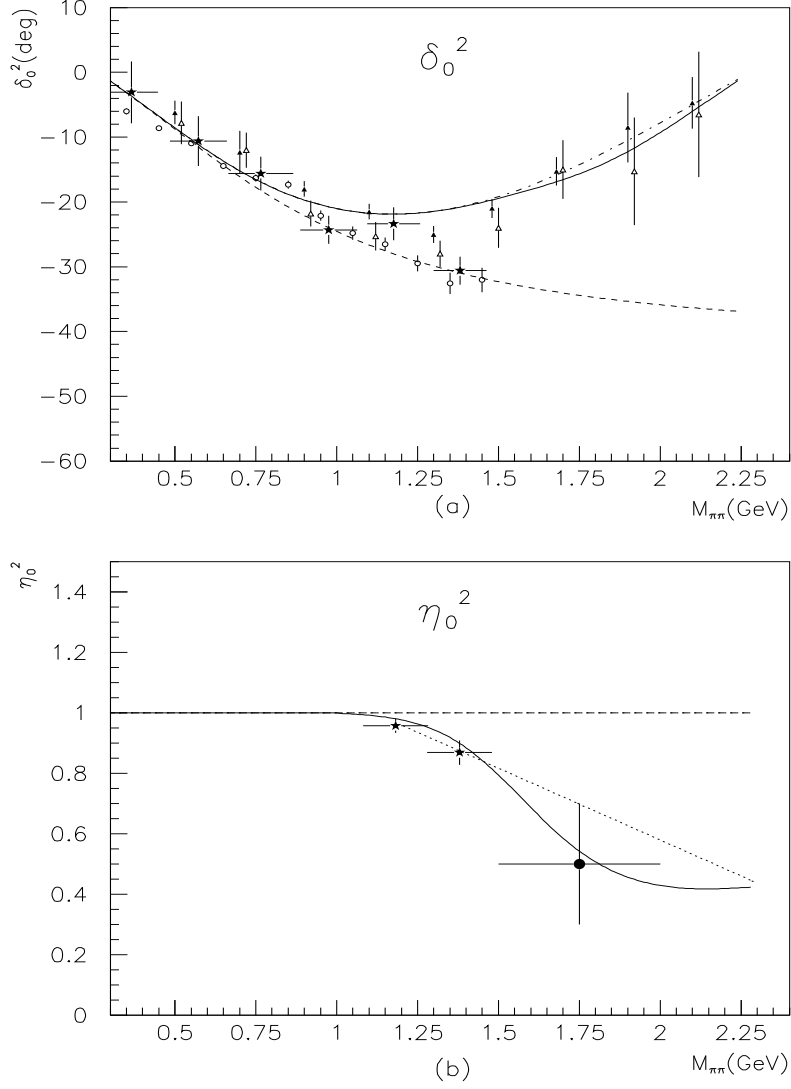
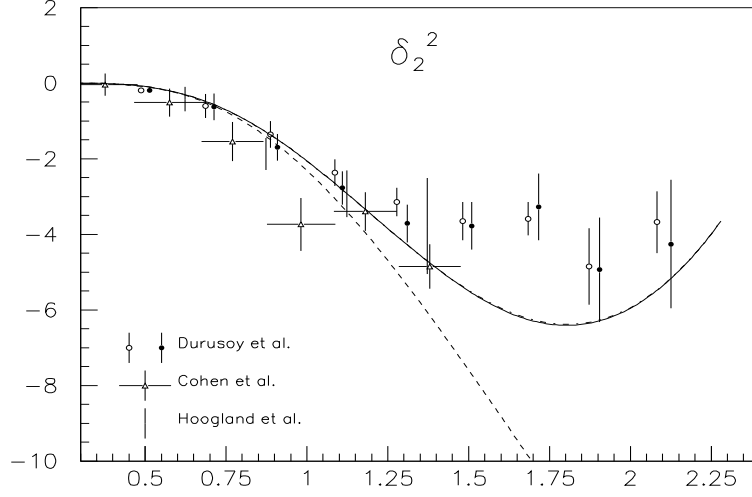
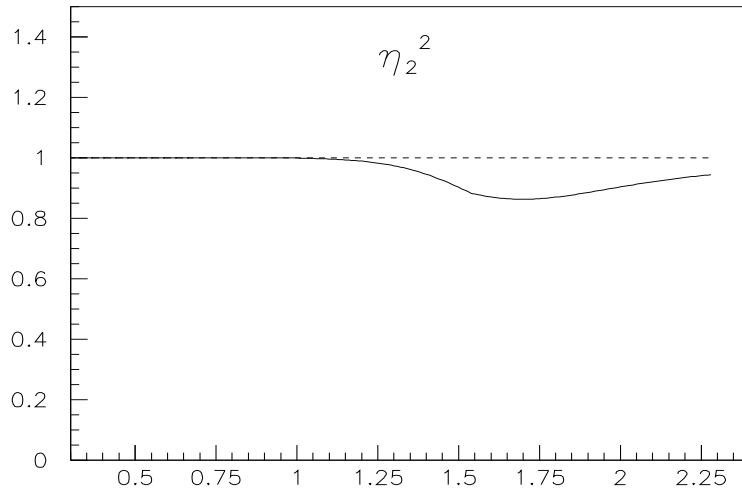


Figure 3: The $I = 2$ $\pi\pi$ S -wave phase shift δ_0^2 (a) and inelastic coefficient η_0^2 (b). The experimental data for δ_0^2 are from Ref.[8] (circles), Ref.[10](stars), and Ref.[9](triangles); the data for η_0^2 are from Ref.[10](stars), and Ref.[9] (solid circle). The solid curves are results including the total contribution from ρ , $f_2(1270)$ exchange and the box diagram. The dot-dashed curves are from ρ and $f_2(1270)$ exchange. The dashed curves include only t-channel ρ exchange. The dotted line in (b) is $\eta_0^2 = 1.53 - 0.475m_{\pi\pi}(GeV/c^2)$ used in Ref.[9].



(a)



(b)

Figure 4: The $I = 2$ $\pi\pi$ D -wave phase shift δ_2^2 (a) and inelastic coefficient η_2^2 (b). The experimental data for δ_2^2 are from Ref.[8] (short lines), Ref.[9](squares), and Ref.[10](triangles). The solid curves represent the total contribution of ρ , $f_2(1270)$ exchange and the box diagram. The dot-dashed curves are from ρ and $f_2(1270)$ exchange. The dashed curves include only t-channel ρ exchange.

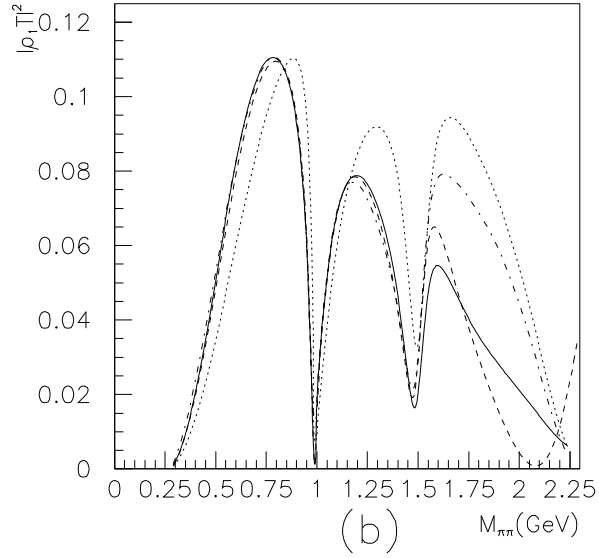
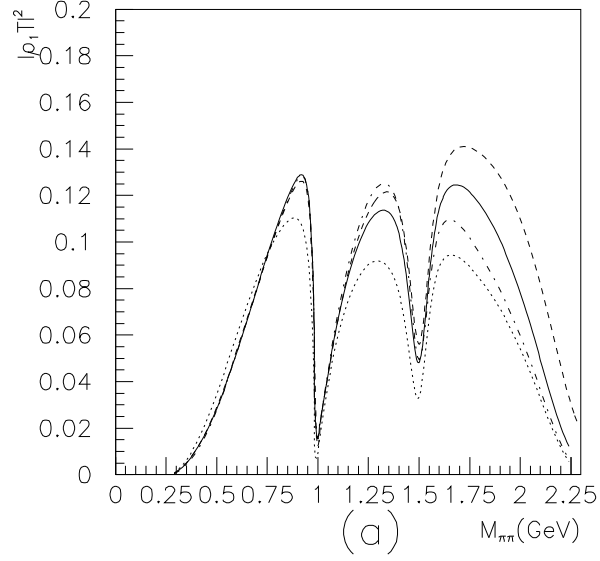


Figure 5: Full amplitudes squared of $\pi^+\pi^- \rightarrow \pi^+\pi^-$ (a) and $\pi^+\pi^- \rightarrow \pi^0\pi^0$ (b). The lines correspond to using $T_s^{I=0}$ from Ref.[12] plus various input of $T_s^{I=2}$: $T_s^{I=2} = 0$ (dotted lines); $T_s^{I=2}$ from Refs.[12, 19] (dot-dashed lines); $T_s^{I=2}$ from Ref.[6] (dashed lines); $T_s^{I=2}$ from this work including t-channel ρ & f_2 exchange and the $\pi\pi \leftrightarrow \rho\rho$ coupled-channel effect.

δ_0^2 and η_0^2 data simultaneously. While the η_0^2 needs the resonance with mass around 1.6 GeV, the δ_0^2 needs the mass above 2.3 GeV with a much broader width.

To demonstrate the significance of possible impact of the $I = 2$ input for the extraction of $I = 0$ $\pi\pi$ amplitude, we calculate the full S-wave amplitudes for $\pi^+\pi^- \rightarrow \pi^+\pi^-$ and $\pi^+\pi^- \rightarrow \pi^0\pi^0$ according to Eqs.(1,2) with $T_s^{I=0}$ from Ref.[12] plus various $T_s^{I=2}$ inputs. The corresponding full S-wave amplitudes squared ($|\rho_1 T|^2$) are shown in Fig.5. The dotted lines are the results with $T_s^{I=2} = 0$. The dot-dashed lines correspond to the scattering length formula for I=2 S-wave as $T_s^{I=2} = a_0 q / (1 - ia_0 q)$ and $a_0 = -0.11 \pm 0.01 m_\pi^{-1}$ as used in Refs.[3, 12, 19], which is similar to the result by considering only the t-channel ρ exchange contribution. The dashed lines use the new empirical $T_s^{I=2}$ formula of Ref.[6], which is similar to the result by considering t-channel ρ and f_2 exchange contributions, but ignoring the inelasticity caused by $\pi\pi \rightarrow \rho\rho \rightarrow \pi\pi$ box diagram contribution. The solid lines are results with our $T_s^{I=2}$ including the t-channel ρ, f_2 exchange and the contribution of the box diagram. It is clear that $T_s^{I=2}$ has significant contribution to the amplitudes for $\pi^+\pi^- \rightarrow \pi^+\pi^-$ and $\pi^+\pi^- \rightarrow \pi^0\pi^0$ processes, hence has significant impact on the extraction of the $T_s^{I=0}$ amplitude. Previous inputs of $T_s^{I=2}$ give similar results as our new $T_s^{I=2}$ for energies below 1.1 GeV, but differ from ours significantly for higher energies. The inclusion of both t-channel f_2 exchange and $\pi\pi \rightarrow \rho\rho \rightarrow \pi\pi$ box diagram contribution is important.

In summary, the basic features of $I = 2$ $\pi\pi$ scattering phase shifts and inelasticities can be well reproduced by the t-channel meson (ρ, f_2) exchange and the $\pi\pi \leftrightarrow \rho\rho$ coupled-channel effect in the K-matrix formalism. The t-channel ρ exchange provides repulsive negative phase shifts while the t-channel $f_2(1270)$ gives an attractive force to increase the phase shifts for $\pi\pi$ scattering above 1 GeV, and the coupled-channel box diagram causes the inelasticities. A correct description of the $I = 2$ $\pi\pi$ scattering has significant impact on the extraction of the $I = 0$ scattering amplitudes from $\pi^+\pi^- \rightarrow \pi^+\pi^-$ and $\pi^+\pi^- \rightarrow \pi^0\pi^0$ data, especially for energies above 1.2 GeV. A re-analysis of these data with our new description of the $I = 2$ $\pi\pi$ scattering will be carried out as our next step.

4 Acknowledgments

The work is partly supported by CAS Knowledge Innovation Project (KJCX2-SW-N02) and the National Natural Science Foundation of China under Grant Nos.10225525,10055003. We thank the Royal Society for funds allowing a collaboration between Queen Mary College, University of London and IHEP, Beijing.

References

- [1] Particle Data Group, Euro. Phys. J. C15 (2001) 1.
- [2] P.Minkovski and W.Ochs, Eur. Phys. J. C9, 283 (1999).
- [3] D.V. Bugg, A.V. Sarantsev, and B.S. Zou, Nucl. Phys. **B 471** (1996) 59.
- [4] B. Ananthanarayan, G. Colangelo, J. Gasser, H. Leutwyler, Phys. Rept. **353** (2001) 207.
- [5] V.V.Anisovich et al., Phys. Lett.**B389** (1996) 388.
- [6] N.N.Achasov, G.N.Shestakov, Phys. Rev. **D67** (2003) 114018.
- [7] B.S.Zou and D.V.Bugg, Phys. Rev. **D48** (1993) 3948.
- [8] W. Hoogland et al., Nucl. Phys. **B 126** (1977) 109.
- [9] N.B.Durusoy et al., Phys. Lett. **45B** (1973) 517.
- [10] D.Cohen, T.Ferbel, P.Slattery, and B.Werner, Phys. Rev.**D7**(1973) 661.
- [11] J.Weinstein and N.Isgur, Phys. Rev. D **41** (1990) 2236; Phys. Rev. Lett. **48** (1982) 659.
- [12] L. Li, B.S. Zou, G.L. Li, Phy. Rev. **D 63** (2001) 074003.
- [13] B.S.Zou and D.V.Bugg, Phys. Rev. **D 50** (1994) 591.
- [14] G.Jansen et al., Phys. Rev. D52 (1995) 2690; D.Lohse et al., Nucl .Phys. **A516** (1990) 513.

- [15] M.P. Locher, V.E. Markushin and H.Q. Zheng, Phys. Rev. **D55** (1997) 2894.
- [16] J.R.Pelaz, J.A.Oller, and E.Oset, Nucl. Phys. **A675** (2000) 92c; J.A.Oller et al., Phys. Rev. Lett. **80** (1998) 3452.
- [17] S.Ishida et al., Prog. Theor. Phys. **95** (1996) 745.
- [18] L. Li, B.S. Zou, G.L. Li, Phy. Rev. **D 67** (2003) 034025.
- [19] B. Hyams et al., Nucl. Phys. **B 64** (1973) 134.
- [20] H. Becker et al., Nucl. Phys. **B151** (1979) 46.
- [21] R.Kaminski et al., Z.Phys. **C74** (1997) 79.
- [22] E852 Colla. (J.Gunter et al.), Phys. Rev. **D64** (2001) 072003.
- [23] GAMS Colla. (D.Alde et al.), Z. Phys.**C66** (1995) 375.
- [24] B.R. Martin, D. Morgan and G. Shaw, *Pion-Pion Interactions in Particle Physics*, Academic, New York, 1974.
- [25] Y.Lu, B.S.Zou and M.P.Locher, Z. Phys. **A345** (1993) 207; M.P.Locher, Y.Lu and B.S.Zou, Z. Phys. **A347** (1994) 281.
- [26] M.E.Peskin, D.V.Schröder, *An Introduction to Quantum Field Theory*, Addison-Wesley Publishing Company, 1995.
- [27] LEPS Colla. (T.Nakano et al.), Phys. Rev. Lett. **91** (2003) 012002.
- [28] V.V.Barmin et al., hep-ex/0304040.
- [29] CLAS Colla. (S.Stepanyan et al.), hep-ex/0307018.
- [30] SAPHIR Colla. (J.Barth et al.), hep-ex/0307083.